PHYSICAL REVIEW D **76,** 115007 (2007)

Pion form factor in the chiral limit of a hard-wall AdS/QCD model

H. R. Grigoryan[1,2] and A. V. Radyushkin[1,3,4]

[1]*Thomas Jefferson National Accelerator Facility, Newport News, Virginia 23606, USA*
[2]*Physics Department, Louisiana State University, Baton Rouge, Louisiana 70803, USA*
[3]*Physics Department, Old Dominion University, Norfolk, Virginia 23529, USA*
[4]*Laboratory of Theoretical Physics, JINR, Dubna, Russian Federation*

(Received 12 September 2007; published 6 December 2007)

We describe a formalism to calculate form factor and charge density distribution of the pion in the chiral limit using the holographic dual model of QCD with hard-wall cutoff. We introduce two conjugate pion wave functions and present analytic expressions for these functions and for the pion form factor. They allow us to relate such observables as the pion decay constant and the pion charge electric radius to the values of chiral condensate and hard-wall cutoff scale. The evolution of the pion form factor to large values of the momentum transfer is discussed, and results are compared to existing experimental data.

DOI: 10.1103/PhysRevD.76.115007 PACS numbers: 11.25.Tq, 11.10.Kk, 11.25.Wx

I. INTRODUCTION

During the last few years applications of gauge/gravity duality [1] to hadronic physics attracted a lot of attention, and various holographic dual models of QCD were proposed in the literature (see, e.g., [2–21]). These models were able to incorporate such essential properties of QCD as confinement and chiral symmetry breaking, and also to reproduce many of the static hadronic observables (decay constants, masses), with values rather close to the experimental ones. Amongst the dual models, a special class is the so-called "bottom-up" approaches (see, e.g., [6–9]), the goal of which is to reproduce known properties of QCD by choosing an appropriate theory in the 5-dimensional (5D) AdS bulk. Within the framework of the AdS/QCD models, by modifying the theory in the bulk one may try to explain/fit experimental results in different sectors of QCD.

In the present paper, we will be interested in the hard-wall AdS/QCD model [6–8], where the confinement is modeled by sharp cutting off the AdS space along the extra fifth dimension at a wall located at some finite distance $z = z_0$. In the framework of this hard-wall model, it is possible to find form factors and wave functions of vector mesons (see, e.g., [22]). To reproduce the general features of the spectrum for the higher states ("linear confinement"), a soft-wall model was proposed in [9]. The ρ-meson form factors for this model were calculated in Ref. [23].

In general, the vector sector is less sensitive to the infrared (IR) effects, since this symmetry is not broken in QCD. However, the axial-vector sector appears to be very sensitive to the particular way the chiral symmetry is broken or, in other words, to the bulk content and the shape of the IR wall [9].

In this respect, one of the interesting objects to study in the holographic dual models of QCD is the pion. The properties of the pion were studied in various holographic approaches, (see e.g. Refs. [5,6,8,12–16,19,21,24]). In particular, the approach of Ref. [6] (see also recent papers [16,19,21]) managed to reproduce the (Gell-Mann—Oakes—Renner) relation $m_\pi^2 \sim m_q$ between the quark mass m_q and mass of the pion m_π and also the $g_{\rho\pi\pi}$ coupling (the coupling between ρ meson and two pions). In Ref. [8], the solution of the pion wave-function equation was explicitly written for the $m_q = 0$ limit.

In this paper, working in the framework of the model proposed in [6] (hard-wall model), we describe a formalism to calculate the form factor and wave functions (and also the density function) of the pion. Since the fits of Ref. [6] give a very small $m_q \sim 2$ MeV value for the explicit chiral symmetry breaking parameter m_q, we consider only the chiral limit $m_q = 0$ of the hard-wall holographic dual model of two-flavor QCD. Resorting to the chiral limit allows us to utilize one of the main advantages of AdS/QCD—the possibility to work with explicit analytic solutions of the basic equations of motion. Expressing the pion form factor in terms of these solutions, we are able, in particular, to extract and analyze the behavior of the pion electric radius in various regions of the holographic parameters space. On the numerical side, we come to the conclusion that the radius of the pion is smaller than what is known from experiment. However, we suggest that, as in case of the radius of the ρ meson, smoothing the IR wall may increase the pion radius.

In our analysis, we introduce and systematically use two types of holographic wave functions $\Phi(z)$ and $\Psi(z)$, which are conjugate to each other and basically similar to the analogous objects introduced in our papers [22,23], where we studied vector mesons.

The paper is organized in the following way. We start with recalling, in Sec. II, the basics of the hard-wall model and some results obtained in Ref. [6], in particular, the form of the relevant action, the eigenvalue equations for bound states and their solutions. In Sec. III, we describe a formalism for calculating the pion form factor and express it in terms of the two wave functions mentioned above. In Sec. IV, we discuss the relation of our AdS/QCD results to

experimental data. We express the values of the pion decay constant and the pion charge radius in terms of the fundamental parameters of the theory and study their behavior in different regions of the parametric space. At the end, we study the behavior of the pion form factor at large momentum transfer. Finally, we summarize the paper.

II. PRELIMINARIES

In the holographic model of hadrons, QCD resonances correspond to Kaluza-Klein (KK) excitations in the sliced AdS_5 background. In particular, vector mesons correspond to the KK modes of transverse vector gauge field in this background. Since the gauge symmetry in the vector sector of the hard-wall model is not broken, the longitudinal component of the vector gauge field is unphysical, and only transverse components correspond to physical mesons. Similarly, the axial-vector mesons are the modes of the transverse part of the axial-vector gauge field. However, because the axial-vector gauge symmetry is broken in the 5D background, the longitudinal components have physical meaning and are related to the pion field. This should be taken into account if we want to treat the pion in a consistent way.

A. Action and equations of motion

The standard prescription of the holographic model is that there is a correspondence between the 4D vector and axial-vector currents and the corresponding 5D gauge fields:

$$\begin{aligned} J^a_{V\mu}(x) &= \bar{q}(x)\gamma_\mu t^a q(x) \to V^a_\mu(x,z) \\ J^a_{A\mu}(x) &= \bar{q}(x)\gamma_\mu\gamma_5 t^a q(x) \to A^a_\mu(x,z), \end{aligned} \tag{1}$$

where $t^a = \sigma^a/2$, ($a = 1, 2, 3$ and σ^a are usual Pauli matrices).

In general, one can write $A = A_\perp + A_\parallel$, where $A_\perp$ and $A_\parallel$ are transverse and longitudinal components of the axial-vector field. The spontaneous symmetry breaking causes $A_\parallel$ to be physical and associated with the Goldstone boson, pion in this case. The longitudinal component may be written in the form: $A^a_{M\parallel}(x,z) = \partial_M \psi^a(x,z)$. Then $\psi^a(x,z)$ corresponds to the pion field. Physics of the axial-vector and pseudoscalar sectors is described by the action

$$S^A_{\rm AdS} = {\rm Tr}\int d^4x dz\Big[\frac{1}{z^3}(D^M X)^\dagger (D_M X) + \frac{3}{z^5}X^\dagger X - \frac{1}{4g_5^2 z}A^{MN}A_{MN}\Big], \tag{2}$$

where $DX = \partial X - iA_L X + iXA_R$, ($A_{L(R)} = V \pm A$) and $X(x,z) = v(z)U(x,z)/2$ is taken as a product of the chiral field $U(x,z) = \exp(2it^a\pi^a(x,z))$ and the function $v(z) = m_q z + \sigma z^3$ containing the chiral symmetry breaking parameters m_q and σ, with m_q playing the role of the quark mass and σ that of the quark condensate. Expanding $U(x,z)$ in powers of π^a gives the relevant piece of the action

$$S^{A(2)}_{\rm AdS} = {\rm Tr}\int d^4x dz\Big[-\frac{1}{4g_5^2 z}A^{MN}A_{MN} + \frac{v^2(z)}{2z^3}(A^a_M - \partial_M\pi^a)^2\Big]. \tag{3}$$

This Higgs-like mechanism breaks the axial-vector gauge symmetry by bringing a z-dependent mass term in the A-part of the Lagrangian. Varying the action with respect to the transverse part of the axial-vector gauge field $A^a_{\perp\mu}(x,z)$ and representing the Fourier image of $A^a_{\perp\mu}(x,z)$ as $\tilde{A}^a_{\perp\mu}(p,z)$ we will get the following equation of motion

$$\Big[z^3\partial_z\Big(\frac{1}{z}\partial_z\tilde{A}^a_\mu\Big) + p^2z^2\tilde{A}^a_\mu - g_5^2v^2\tilde{A}^a_\mu\Big]_\perp = 0, \tag{4}$$

that determines physics of the axial-vector mesons, like A_1. The axial-vector bulk-to-boundary propagator $\mathcal{A}(p,z)$ is introduced by the relation $\tilde{A}^a_{\perp\mu}(p,z) = \mathcal{A}(p,z)A^a_\mu(p)$. It satisfies Eq. (4) with boundary conditions (b.c.) $\mathcal{A}(p,0) = 1$ and $\mathcal{A}'(p,z_0) = 0$. Similarly, variation with respect to the longitudinal component $\partial_\mu\psi^a$ gives

$$z^3\partial_z\Big(\frac{1}{z}\partial_z\psi^a\Big) - g_5^2v^2(\psi^a - \pi^a) = 0. \tag{5}$$

Finally, varying with respect to A_z produces

$$p^2z^2\partial_z\psi^a - g_5^2v^2\partial_z\pi^a = 0. \tag{6}$$

The pion wave function is determined from Eqs. (5) and (6) with b.c. $\partial_z\psi(z_0) = 0$, $\psi(\epsilon) = 0$ and $\pi(\epsilon) = 0$.

Within the framework of the model of Ref. [6], it is possible to derive the Gell-Mann—Oakes—Renner relation $m_\pi^2 \sim m_q$ producing massless pion in the $m_q = 0$ limit. Taking $p^2 = m_\pi^2$ in Eq. (6) gives

$$\partial_z\pi = \frac{m_\pi^2 z^2}{g_5^2v^2}\partial_z\psi. \tag{7}$$

A perturbative solution in the form of m_π^2 expansion was proposed in Ref. [6], with $\psi(z) = \mathcal{A}(0,z) - 1$ in the lowest order. Then it was shown that, in the $m_q \to 0$ limit, $\pi(z)$ tends to $-\theta(z - z_0)$ or, roughly speaking, $\pi = -1$ in this limit. Since our goal is to calculate the pion form factor in the chiral limit, this approximation will be sufficient for us.

B. Two-point function

The spectrum in the axial-current channel consists of the pseudoscalar pion $\langle 0|J_A^\alpha|\pi(p)\rangle = if_\pi p^\alpha$ and axial-vector mesons $\langle 0|J_A^\alpha|A_n(p,s)\rangle = F_{A,n}\epsilon_n^\alpha(p,s)$, where $F_{A,n}$ corresponds to the nth axial-vector meson decay constant (and we ignored the flavor indexes). Thus, the two-point function for the axial-vector currents has the form:

$$\langle J_A^\alpha(p)J_A^\beta(-p)\rangle = p^\alpha p^\beta \frac{f_\pi^2}{p^2} + \sum_n \Pi_n^{\alpha\beta}(p)\frac{F_{A,n}^2}{p^2 - M_{A,n}^2}. \tag{8}$$

where the meson polarization tensor is given by

$$\Pi_n^{\alpha\beta}(p) = \sum_s \epsilon_n^\alpha(p,s)\epsilon_n^\beta(p,s) = -\eta^{\alpha\beta} + \frac{p^\alpha p^\beta}{M_{A,n}^2}. \tag{9}$$

The representation for the two-point function can be also written as

$$\langle J_A^\alpha(p)J_A^\beta(-p)\rangle = p^\alpha p^\beta \frac{f_\pi^2}{p^2} + \left(-\eta^{\alpha\beta} + \frac{p^\alpha p^\beta}{p^2}\right) \times \sum_n \frac{F_{A,n}^2}{p^2 - M_{A,n}^2} + (\text{nonpole terms}), \tag{10}$$

in which the second term on the rhs is explicitly transverse to p.

As noted in Ref. [6], using holographic correspondence one can relate the two-point function to $[\partial_z A(p,z)/z]_{z=0}$ and derive that

$$f_\pi^2 = -\frac{1}{g_5^2}\left(\frac{1}{z}\partial_z A(0,z)\right)_{z=\epsilon\to 0}. \tag{11}$$

For large spacelike p^2, Eq. (4) gives the same solution as in case of vector mesons, and the same asymptotic logarithmic behavior, just as expected from QCD.

C. Pion wave functions

The longitudinal component of the axial-vector gauge field was defined as $A_\parallel = \partial\psi$. In the chiral limit, when $p^2 = m_\pi^2 = 0$, we have $\partial_z\pi = 0$, and the basic equation for ψ, Eq. (5) can be rewritten as the equation

$$z^3\partial_z\left(\frac{1}{z}\partial_z\Psi\right) - g_5^2 v^2\Psi = 0 \tag{12}$$

for the function $\Psi \equiv \psi - \pi$. In the chiral limit, when $\pi(z) \to -1$, the value of $\Psi(\epsilon)$ tends to 1 as $\epsilon \to 0$. This value and the b.c. $\Psi'(z_0) = 0$ are the same as those for $\mathcal{A}(p,z)$ and, furthermore, Eq. (12) coincides with the $p^2 = 0$ version of Eq. (4) for $\mathcal{A}(p,z)$. Hence, the solution for $\Psi(z)$ coincides with $\mathcal{A}(0,z)$:

$$\Psi(z) = \mathcal{A}(0,z), \tag{13}$$

and we may write

$$f_\pi^2 = -\frac{1}{g_5^2}\left(\frac{1}{z}\partial_z\Psi(z)\right)_{z=\epsilon\to 0}. \tag{14}$$

In our analysis of ρ-meson wave functions in Refs. [22,23], we emphasized that it makes sense to consider also the conjugate functions $\Phi(z) \sim \Psi'(z)/z$ of the corresponding Sturm-Liouville equation. As we observed, they are closer in their structure to the usual quantum mechanical bound state wave functions than the solutions of the original equation. In the pion case, it is convenient to define the Φ function as

$$\Phi(z) = -\frac{1}{g_5^2 f_\pi^2}\left(\frac{1}{z}\partial_z\Psi(z)\right). \tag{15}$$

It vanishes at the IR boundary $z = z_0$ and, according to Eq. (11), is normalized as

$$\Phi(0) = 1 \tag{16}$$

at the origin. Note also that using Eq. (12) we can express Ψ as derivative of Φ:

$$\Psi(z) = -\frac{f_\pi^2 z^3}{v^2}\partial_z\Phi(z). \tag{17}$$

III. EXTRACTING PION ELECTROMAGNETIC FORM FACTOR

A. Three-point function

To obtain the pion form factor, we need to consider three-point correlation functions. The correlator should include the external EM current $J_\mu^{el}(0)$ and currents having nonzero projection onto the pion states, e.g. the axial currents $J_{5\alpha}^a(x_1)$, $J_{5\beta}^{a\dagger}(x_2)$

$$\mathcal{T}_{\mu\alpha\beta}(p_1,p_2) = \int d^4x_1 \int d^4x_2 e^{ip_1x_1 - ip_2x_2} \times \langle 0|\mathcal{T}J_{5\beta}^\dagger(x_2)J_\mu^{\text{el}}(0)J_{5\alpha}(x_1)|0\rangle, \tag{18}$$

where p_1, p_2 are the corresponding momenta, with the momentum transfer carried by the EM source being $q = p_2 - p_1$ (as usual, we denote $q^2 = -Q^2$, $Q^2 > 0$). The spectral representation for the three-point function is a two-dimensional generalization of Eq. (8)

$$\mathcal{T}^{\mu\alpha\beta}(p_1,p_2) = p_1^\alpha p_2^\beta (p_1 + p_2)^\mu \frac{f_\pi^2 F_\pi(Q^2)}{p_1^2 p_2^2} + \sum_{n,m}(\text{transverse terms}) + (\text{nonpole terms}), \tag{19}$$

where the first term, longitudinal both with respect to p_1^α and p_2^β contains the pion electromagnetic form factor $F_\pi(Q^2)$

$$\langle\pi(p_1)|J_\mu^{el}(0)|\pi(p_2)\rangle = F_\pi(q^2)(p_1 + p_2)_\mu, \tag{20}$$

(normalized by $F_\pi(0) = 1$), while other pole terms contain the contributions involving axial-vector mesons and are transverse either with respect to p_1^α or p_2^β, or both. Hence, the pion form factor can be extracted from the three-point function using

$$p_{1\alpha} p_{2\beta} \mathcal{T}^{\mu\alpha\beta}(p_1, p_2)|_{p_1^2=0, p_2^2=0} = (p_1 + p_2)^\mu f_\pi^2 F_\pi(Q^2). \tag{21}$$

B. Trilinear terms in F^2 part of action

To obtain form factor from the holographic model, we need the action of the third order in the fields. There are two types of terms contributing to the pion electromagnetic form factor: $|DX|^2$ term and F^2 terms. Let us consider first the contribution from F^2 terms. They contain VVV, VAA, and AVA interactions and may be written as

$$S_{\rm AdS}^{F^2}|_3 = \frac{i}{g_5^2} \mathrm{Tr} \int d^4x dz \frac{1}{z} (V_{MN}[V^M, V^N] + V_{MN}[A^M, A^N] + A_{MN}[V^M, A^N]), \tag{22}$$

where $V_{MN} = \partial_M V_N - \partial_N V_M$ and $A_{MN} = \partial_M A_N - \partial_N A_M$. Taking $V_z = A_z = 0$ gauge, we pick out the part of the action which is contributing to the 3-point function $\langle J_{5\alpha} J_\mu J_{5\beta} \rangle$:

$$W_3 = \frac{i}{g_5^2} \mathrm{Tr} \int d^4x dz \frac{1}{z} (V_{\mu\nu}[A^\mu, A^\nu] + A_{\mu\nu}[V^\mu, A^\nu]). \tag{23}$$

Introducing Fourier transforms of fields, we define, as usual, $V_\mu(q, z) = \tilde{V}_\mu(q) \mathcal{V}(q, z)$ for the vector field, where $\tilde{V}_\mu(q)$ is the Fourier transform of the 4-dimensional field $V_\mu(x)$ and $\mathcal{V}(q, z)$ is the bulk-to-boundary propagator satisfying the equation

$$z\partial_z \left(\frac{1}{z} \partial_z \mathcal{V}(q, z) \right) + q^2 \mathcal{V}(q, z) = 0 \tag{24}$$

with b.c. $\mathcal{V}(q, 0) = 1$ and $\partial_z \mathcal{V}(q, z_0) = 0$. It can be written as the sum

$$\mathcal{V}(q, z) = g_5 \sum_{m=1}^{\infty} \frac{f_m \psi_m^V(z)}{-q^2 + M_m^2} \tag{25}$$

involving all the bound states in the q-channel, with M_m being the mass of the mth bound state and $\psi_m^V(z)$ its wave function given by a solution of the basic equation of motion in the vector sector.

The projection (21) picks out only the longitudinal part $A_{\|\mu}(p, z)$ of the axial-vector field. Taking into account that $A_{\|\mu}^a(x, z) = \partial_\mu \psi(x, z)$, we may write

$$A_{\|\mu}^a(p, z) = i p_\mu \psi^a(p, z), \tag{26}$$

where $A_{\|\mu}^a(p, z)$ and $\psi^a(p, z)$ are the Fourier transforms of $A_{\|\mu}^a(x, z)$ and $\psi(x, z)$, respectively. Furthermore, there is only one particle in the expansion over bound state in this case, namely, the massless pion. Thus, we have $A_{\|\mu}^a(p, z) = \tilde{A}_{\|\mu}^a(p) \psi(z)$ and, therefore,

$$\psi^a(p, z) = -\frac{i p^\alpha}{p^2} \tilde{A}_{\|\alpha}^a(p) \psi(z). \tag{27}$$

This allows us to rewrite $A_{\|\mu}^a(p, z)$ in the form

$$A_{\|\mu}^a(p, z) = \frac{p^\alpha p_\mu}{p^2} \tilde{A}_{\|\alpha}^a(p) \psi(z) \tag{28}$$

involving the longitudinal projector $p^\alpha p_\mu / p^2$ and the pion wave function $\psi(z)$, which is the solution of the basic equation (5). Using this representation and making Fourier transform of W_3 gives

$$\begin{aligned} W_3 = & -\frac{1}{2g_5^2} \epsilon_{abc} \int \frac{d^4u d^4v d^4w}{(2\pi)^{12}} i(2\pi)^4 \delta^{(4)}(u + v + w) \\ & \times \frac{u^\mu v^\nu u^\alpha v^\beta}{u^2 v^2} \tilde{A}_{\|\alpha}^b(u) \tilde{A}_{\|\beta}^c(v) [w_\mu \tilde{V}_\nu^a(w) - w_\nu \tilde{V}_\mu^a(w)] \\ & \times \int_\epsilon^{z_0} dz \frac{1}{z} \mathcal{V}(w, z) \psi^2(z) \end{aligned} \tag{29}$$

[notice that the second term in Eq. (23) vanishes for longitudinal axial-vector fields]. Varying this functional with respect to sources produces the following 3-point function:

$$\begin{aligned} & \langle J_{V,a}^\mu(q) J_{\|A,b}^\alpha(p_1) J_{\|A,c}^\beta(-p_2) \rangle \\ & = -i(2\pi)^4 \delta^{(4)}(q + p_1 - p_2) \epsilon_{abc} \frac{p_1^\alpha p_2^\beta}{p_1^2 p_2^2} (p_1 + p_2)^\mu \\ & \quad \times \frac{1}{2g_5^2} q^2 \int_\epsilon^{z_0} dz \frac{1}{z} \mathcal{V}(q, z) \psi^2(z), \end{aligned} \tag{30}$$

where, anticipating the limit $p_1^2 \to 0$, $p_2^2 \to 0$, we took $(p_1 q) = -(p_2 q) = -q^2/2$ in the numerator factors. Now, representing $\langle J_{V,a}^\mu(q) J_{\|A,b}^\alpha(p_1) J_{\|A,c}^\beta(-p_2) \rangle = i(2\pi)^4 \delta^{(4)}(q + p_1 - p_2) \epsilon_{abc} \mathcal{T}^{\mu\alpha\beta}(p_1, p_2)$ and applying the projection suggested by Eq. (21), we will have

$$\begin{aligned} & \lim_{p_1^2 \to 0} \lim_{p_2^2 \to 0} p_{1\alpha} p_{2\beta} \mathcal{T}^{\mu\alpha\beta}(p_1, p_2) \\ & = \frac{1}{2g_5^2} (p_1 + p_2)^\mu Q^2 J(Q), \end{aligned} \tag{31}$$

where $J(Q)$ is the dynamic factor given by the convolution

$$J(Q) = \int_\epsilon^{z_0} \frac{dz}{z} \mathcal{J}(Q, z) \psi^2(z). \tag{32}$$

C. Dynamic factor and wave functions

The vector bulk-to-boundary propagator $\mathcal{J}(Q,z) \equiv \mathcal{V}(iQ,z)$ for spacelike momenta, entering into the dynamic factor $J(Q)$, satisfies the equation

$$z\partial_z\left(\frac{1}{z}\,\partial_z\mathcal{J}(Q,z)\right) = Q^2\mathcal{J}(Q,z) \tag{33}$$

with b.c. $\mathcal{J}(Q,0)=1$ and $\partial_z\mathcal{J}(Q,z_0)=0$. Its explicit form is given by

$$\mathcal{J}(Q,z) = Qz\left[K_1(Qz) + I_1(Qz)\frac{K_0(Qz_0)}{I_0(Qz_0)}\right]. \tag{34}$$

One can easily see that $\mathcal{J}(0,z)=1$. Combining all the factors, we get

$$f_\pi^2 F_\pi^{(F^2)}(Q^2) = \frac{1}{2g_5^2}Q^2\int_0^{z_0}\frac{dz}{z}\,\mathcal{J}(Q,z)\psi^2(z). \tag{35}$$

Integrating by parts and using equations of motion both for $\mathcal{J}$ and ψ gives

$$F_\pi^{(F^2)}(Q^2) = \frac{1}{g_5^2 f_\pi^2}\int_0^{z_0} dz z\mathcal{J}(Q,z) \times\left[\left(\frac{\partial_z\psi}{z}\right)^2 + \frac{g_5^2 v^2}{z^4}\psi(\psi-\pi)\right]. \tag{36}$$

We need also to add the $V\pi\pi$ contribution from the $|DX|^2$ term of the AdS action (2). It is generated by

$$S_{\rm AdS}^{|DX|^2}|_{V\pi\pi} = \epsilon_{abc}\int d^4x dz\left[\frac{v^2(z)}{z^3}(A_M^a - \partial_M\pi^a)\pi^b V^{cM}\right], \tag{37}$$

and its inclusion changes $\psi(\psi-\pi)$ into $(\psi-\pi)^2$ in Eq. (36). The total result (see also Ref. [6]) may be now conveniently expressed in terms of the $\Psi \equiv \psi - \pi$ wave function

$$F_\pi(Q^2) = \frac{1}{g_5^2 f_\pi^2}\int_0^{z_0} dz z\mathcal{J}(Q,z)\left[\left(\frac{\partial_z\Psi}{z}\right)^2 + \frac{g_5^2 v^2}{z^4}\Psi^2(z)\right]. \tag{38}$$

Using equation of motion for $\Psi(z)$, one can see that the expression in square brackets coincides with

$$\frac{1}{z}\partial_z\left(\Psi(z)\frac{1}{z}\partial_z\Psi(z)\right) = -g_5^2 f_\pi^2\frac{1}{z}\partial_z(\Psi(z)\Phi(z)),$$

and write the form factor as

$$F_\pi(Q^2) = -\int_0^{z_0} dz\mathcal{J}(Q,z)\partial_z(\Psi(z)\Phi(z)). \tag{39}$$

This representation allows one to easily check the normalization

$$F_\pi(0) = -\int_0^{z_0} dz\partial_z(\Psi(z)\Phi(z)) = \Psi(0)\Phi(0) = 1, \tag{40}$$

where we took into account that $\mathcal{J}(0,z)=1$ and $\Phi(z_0)=0$. We can also represent our result for the pion form factor as

$$F_\pi(Q^2) = \int_0^{z_0} dz z\mathcal{J}(Q,z)\left[g_5^2 f_\pi^2\Phi^2(z) + \frac{\sigma^2}{f_\pi^2}z^2\Psi^2(z)\right] \equiv \int_0^{z_0} dz z\mathcal{J}(Q,z)\rho(z), \tag{41}$$

and interpret the function $\rho(z)$ as the radial distribution density, as it was done in Refs. [22,23]. Note that keeping only the first term in square brackets gives an expression similar to our result [22] for the ρ-meson form factor

$$\mathcal{F}_{11}(Q^2) = \int_0^{z_0} dz z\mathcal{J}(Q,z)|\phi_1(z)|^2 \tag{42}$$

in terms of the function ϕ_1 conjugate to the solution of the basic equation of motion. The value of $\phi_1(z)$ at the origin is proportional to the ρ-meson decay constant $f_\rho/m_\rho \equiv g_\rho$ (experimentally, $g_\rho^{\rm exp} \approx 207$ MeV [25]), namely, $\phi_1(0) = g_5 g_\rho$. Thus, the pion wave function $g_5 f_\pi\Phi(z) \equiv \phi_\pi(z)$ is a direct analog of the ρ-meson wave function $\phi_1(z)$. The main difference is that, in the pion case, there is also the second term in the form factor expression. The latter, in fact, is necessary to secure correct normalization of the form factor at $Q^2=0$. In Eq. (38), this term is written in terms of the $\Psi(z)$ wave function, but using Eq. (17) we can rewrite it also in terms of $\Phi(z)$ or $\phi_\pi(z)$:

$$\rho(z) = \phi_\pi^2(z) + \frac{1}{g_5^2\sigma^2}\left(\frac{1}{z^2}\partial_z\phi_\pi(z)\right)^2. \tag{43}$$

IV. WAVE FUNCTIONS AND FORM FACTOR

A. Structure of pion wave functions

Explicit form of the Ψ wave function follows from the solution of Eq. (12):

$$\Psi(z) = z\Gamma[2/3]\left(\frac{\alpha}{2}\right)^{1/3}\left[I_{-1/3}(\alpha z^3) - I_{1/3}(\alpha z^3)\frac{I_{2/3}(\alpha z_0^3)}{I_{-2/3}(\alpha z_0^3)}\right], \tag{44}$$

where $\alpha = g_5\sigma/3 \approx 1.481\sigma$ (recall that $g_5 = \sqrt{2}\pi$, see e.g. Ref. [23]). As a result, $\Phi(z)$ is given by

$$\Phi(z) = -\frac{1}{g_5^2 f_\pi^2}\left(\frac{1}{z}\partial_z \Psi(z)\right) = \frac{3z^2}{g_5^2 f_\pi^2}\Gamma[2/3]\left(\frac{\alpha^4}{2}\right)^{1/3}\left[-I_{2/3}(\alpha z^3) + I_{-2/3}(\alpha z^3)\frac{I_{2/3}(\alpha z_0^3)}{I_{-2/3}(\alpha z_0^3)}\right]. \tag{45}$$

This formula, combined with Eq. (16), establishes the relation

$$f_\pi^2 = 3\cdot 2^{1/3}\frac{\Gamma[2/3]}{\Gamma[1/3]}\frac{I_{2/3}(\alpha z_0^3)}{I_{-2/3}(\alpha z_0^3)}\frac{\alpha^{2/3}}{g_5^2} \tag{46}$$

for f_π in terms of the condensate parameter α and the confinement radius z_0. Since σ appears in the solutions only through α, we will use α in what follows. Note also that $\alpha^{1/3} \approx 1.14\sigma^{1/3}$.

Realizing that the equations of motion for the vector sector in this holographic model are not affected by the chiral symmetry-breaking effects expressed through the function $v(z)$, it is natural to set the value of z_0 from the vector sector spectrum, i.e., by the ρ-meson mass. The numerical value of z_0 (call it z_0^ρ) is then $z_0^\rho \approx 1/323$ MeV. As given by Eq. (46), f_π looks like a rather complicated function of two scales, z_0 and α. Note, however, that the ratio $I_{2/3}(a)/I_{-2/3}(a)$ is very close to 1 for $a \gtrsim 2$ and practically indistinguishable from 1 for $a \gtrsim 3$. Hence, for sufficiently large values of the confinement radius, $z_0 \gtrsim 1/\alpha^{1/3}$, the value of f_π is determined by the value of α alone. This limiting value of f_π is given by

$$f_\pi|_{z_0\to\infty} = 2^{1/6}\frac{\alpha^{1/3}}{g_5}\sqrt{\frac{3\Gamma[2/3]}{\Gamma[1/3]}} = \frac{3^{1/2}}{2^{1/3}\pi}\sqrt{\frac{\Gamma[2/3]}{\Gamma[1/3]}}\alpha^{1/3} \approx \frac{\alpha^{1/3}}{3.21}. \tag{47}$$

Requiring that $f_\pi|_{z_0\to\infty}$ coincides with the experimental value, $f_\pi \approx 131$ MeV, one should take $\alpha^{1/3} \approx 420$ MeV. For such α, the value of $1/\alpha^{1/3}$ is close to z_0^ρ, i.e., we are in the region $\alpha z_0^3 \sim 1$ and we may expect that, even if we use exact formula (46) with $z_0 = z_0^\rho$, the value of f_π would not change much. Indeed, to get $f_\pi \approx 131$ MeV from Eq. (46) for $1/z_0 = 323$ MeV, we should take $\alpha^{1/3} \approx 424$ MeV $\equiv \alpha_0^{1/3}$. Thus, in this range of parameters, the value of f_π is practically in one-to-one correspondence with the value of α. It is convenient to introduce a dimensionless variable

$$a \equiv \alpha z_0^3 = \tfrac{1}{3}g_5\sigma z_0^3. \tag{48}$$

Then the values $\alpha_0^{1/3} = 424$ MeV and $1/z_0^\rho = 323$ MeV correspond to $a = 2.26 \equiv a_0$. As one can see from Fig. 1, the dependence of f_π on a is practically flat for $a \gtrsim 2$.

The confinement radius z_0 presents a natural scale to measure length, so it makes sense to rewrite the form factor formula (38) as an integral over the dimensionless variable $\zeta \equiv z/z_0$:

$$F_\pi(Q^2) = 3\int_0^1 d\zeta\zeta\mathcal{J}(Q,\zeta,z_0)\left[n(a)\varphi^2(\zeta,a) + \frac{a^2\zeta^2}{n(a)}\psi^2(\zeta,a)\right] \equiv \int_0^1 d\zeta\zeta\mathcal{J}(Q,\zeta,z_0)\rho(\zeta,a), \tag{49}$$

where the mass scale α is reflected by the dimensionless parameter a. The factor $n(a)$ takes care of the correct normalization of the form factor. It is given by

$$n(a) = 2^{1/3}a^{2/3}\frac{\Gamma[2/3]}{\Gamma[1/3]}\frac{I_{2/3}(a)}{I_{-2/3}(a)}. \tag{50}$$

For small a, it may be approximated by $\frac{3}{4}a^2$. For large a, using the fact that $I_{2/3}(a)/I_{-2/3}(a)$ is very close to 1 for $a \gtrsim 2$, we may approximate $n(a) \approx 0.637a^{2/3}$ in this region. In terms of $n(a)$, the pion decay constant can be written as

$$f_\pi = \frac{1}{\pi a^{1/3}}\sqrt{\frac{3}{2}n(a)}\alpha^{1/3}. \tag{51}$$

For large a, this gives

$$f_\pi|_{a\gtrsim 2} \approx 0.311\alpha^{1/3}. \tag{52}$$

For small a, we have

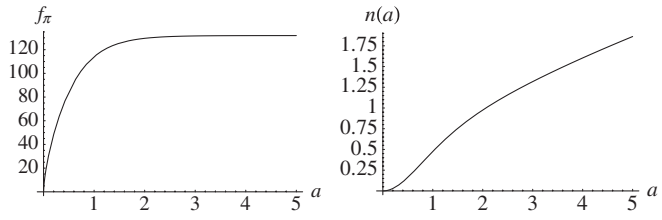

FIG. 1. Left: Pion decay constant f_π as a function of a for fixed $\alpha^{1/3} = 424$ MeV. Right: Function $n(a)$

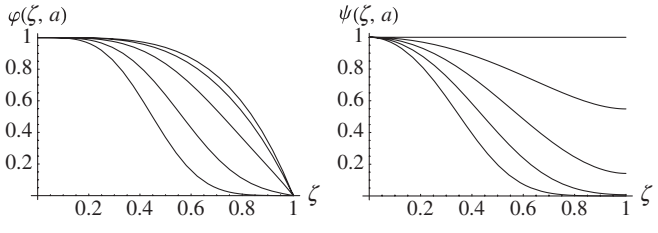

FIG. 2. Functions $\varphi(\zeta, a)$ (left) and $\psi(\zeta, a)$ (right) for several values of a: $a = 0$ (uppermost lines), $a = 1$, $a = 2.26$, $a = 5$, $a = 10$ (lowermost lines).

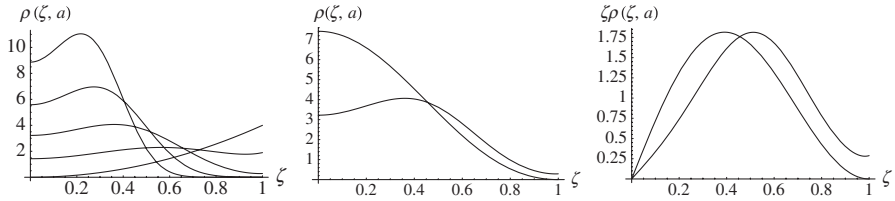

FIG. 3. Left: Function $\rho(\zeta, a)$ for $a = 0$, $a = 1$, $a = 2.26$, $a = 5$, $a = 10$. Middle: Densities $\rho(\zeta, 2.26)$ for pion and $\rho_\rho(\zeta)$ for ρ-meson in the hard-wall model. Right: Same for densities multiplied by ζ.

$$f_\pi|_{a\lesssim 1} = \frac{3a^{2/3}}{2\sqrt{2}\pi}\alpha^{1/3} + \ldots \approx 0.338\alpha z_0^2 = 0.338\frac{a}{z_0}. \tag{53}$$

The functions $\varphi(\zeta, a)$, $\psi(\zeta, a)$ are just the Φ and Ψ wave functions written in ζ and a variables. For $a = 0$, the limiting forms are $\varphi(\zeta, 0) = 1 - \zeta^4$ and $\psi(\zeta, 0) = 1$. As a increases, both functions become more and more narrow (see Fig. 2).

For density, we have $\rho(\zeta, a = 0) = 4\zeta^2$ in the $a \to 0$ limit, a function that vanishes at the origin (see Fig. 3). For nonzero a, the value of $\rho(\zeta = 0, a)$ monotonically increases with a, and the function itself narrows.

The increase of $\rho(\zeta = 0, a)$ with a is generated by the monotonically increasing function $n(a)$. It is interesting to compare the pion density $\rho(\zeta, 2.26)$ (taken at the "experimental" value $a = 2.26$) with the ρ-meson density $\rho_\rho(\zeta)$ of Ref. [22]. These densities are rather close for $\zeta > 0.5$, but strongly differ for small ζ. In particular, the ρ-meson density is more than 2 times larger for $\zeta = 0$, which corresponds to the hard-wall model result that g_ρ is essentially larger than f_π.

B. Pion charge radius

It is interesting to investigate how well these values $z_0 = 1/323$ MeV and $\alpha = (424\ \text{MeV})^3$ describe another important low-energy characteristics of the pion—its charge radius. Using the Q^2-expansion of the vector source [22]

$$\mathcal{J}(Q, \zeta, z_0) = 1 - \frac{Q^2}{4}z_0^2\zeta^2[1 - 2\ln\zeta] + \ldots \tag{54}$$

and explicit form of the density

$$\rho(\zeta, a) = \frac{3}{2}\Gamma(1/3)\Gamma(2/3)a^2\zeta^4\left[\left(\nu(a)I_{-2/3}(a\zeta^3) - \frac{I_{2/3}(a\zeta^3)}{\nu(a)}\right)^2 + \left(\frac{I_{-1/3}(a\zeta^3)}{\nu(a)} - \nu(a)I_{1/3}(a\zeta^3)\right)^2\right], \tag{55}$$

where $\nu(a) \equiv \sqrt{I_{2/3}(a)/I_{-2/3}(a)}$, we obtain for the pion charge radius:

$$\langle r_\pi^2\rangle = \frac{3}{2}z_0^2\int_0^1 d\zeta\zeta^3[1 - 2\ln\zeta]\rho(\zeta, a) = \frac{4}{3}z_0^2\left\{1 - \frac{a^2}{4} + \mathcal{O}(a^4)\right\}. \tag{56}$$

Hence, for fixed z_0 and small a, when $\alpha \ll 1/z_0^3$, the pion radius is basically determined by the confinement scale z_0. In particular, $\langle r_\pi^2\rangle = \frac{4}{3}z_0^2$ for $\alpha = 0$. Numerically, taking $z_0 = z_0^\rho \approx 1/323$ MeV $= 0.619$ fm, we obtain $\langle r_\pi^2\rangle = 0.51$ fm^2. This result is very close to the value $\langle r_\rho^2\rangle_C \approx 0.53$ fm^2 that we obtained in the hard-wall model for the ρ-meson electric radius determined in [22] from the slope of the $G_C(Q^2)$ form factor. However, since $G_C(Q^2)$ involves kinematic-type terms Q^2/m_ρ^2, it seems more appropriate to compare $F_\pi(Q^2)$ with the $\mathcal{F}_{11}(Q^2)$ form factor (42) given directly by a wave function overlap integral. The slope of $\mathcal{F}_{11}(Q^2)$ is smaller than that of $G_C(Q^2)$, and the corresponding radius is also smaller: $\langle r_\rho^2\rangle_\mathcal{F} = 0.27$ fm^2. Thus, for $\alpha = 0$, the pion r.m.s. radius is about 1.4 times larger than the ρ-meson size determined by $\langle r_\rho^2\rangle_\mathcal{F}^{1/2}$.

With the increase of α, the pion becomes smaller (see Fig. 4). The experimental value of 0.45 fm^2 [25] is reached for $a \sim 0.9$. However, the corresponding value $f_\pi \approx 80$ MeV is too small. If we take $a = a_0 = 2.26$, then $\langle r_\pi^2\rangle = 0.34$ fm^2. Thus, if we insist on using $z_0 = z_0^\rho$ dictated by the hard-wall model calculation of the ρ-meson mass, and the value of α producing the experimental f_π (note that then $\alpha^{-2/3} \approx 0.222$ fm^2), the pion radius is smaller than the experimental value. In linear units, the difference, in fact, does not look very drastic: just 0.58 fm instead of 0.66 fm. Given that the hard-wall model for

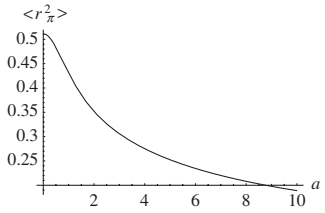

FIG. 4. $\langle r_\pi^2\rangle$ in fm^2 for $z_0 = z_0^\rho$ as a function of a.

confinement is rather crude, the agreement may be considered as encouraging. Furthermore, one may expect that, in a more realistic softer model of confinement, the size of the pion will be larger. Such an expectation is supported by our soft-wall model calculation of the ρ-meson electric radius, for which we obtained $\langle r_\rho^2\rangle_C = 0.66$ fm^2 (0.40 fm^2 for $\langle r_\rho^2\rangle_{\mathcal{F}}$), i.e., the result by 0.13 fm^2 larger than in the hard-wall model. If $\langle r_\pi^2\rangle$ would increase by a similar amount, the result will be very close to the quoted experimental value.

To find $\langle r_\pi^2\rangle$ for large a (i.e., when $\alpha \gtrsim z_0^{-3}$ for fixed z_0, or when $z_0 \gtrsim \alpha^{-1/3}$ for fixed α), we use first the observation that, in the region $a \gtrsim 2$, we may approximate $\nu(a) \approx 1$. Then the factor in square brackets in Eq. (55) becomes a function of the combination $a\zeta^3 \equiv \mu$ [call it $R(\mu)$], and we can write

$$\langle r_\pi^2\rangle|_{a\gtrsim 2} \approx \frac{3}{4}\Gamma(1/3)\Gamma(2/3)\left(\frac{1}{\alpha}\right)^{2/3}\int_0^a d\mu\,\mu^{5/3}R(\mu)\left[1-\frac{2}{3}\ln\frac{\mu}{a}\right]. \tag{57}$$

For $a \gtrsim 2$, the upper limit of integration in this expression may be safely substituted by infinity producing

$$\int_0^\infty d\mu\,\mu^{5/3}R(\mu) = \frac{2^{2/3}}{3\Gamma^2(2/3)} \equiv G, \qquad \int_0^\infty d\mu\,\mu^{5/3}R(\mu)\ln\mu \approx G\ln 0.566, \tag{58}$$

which gives

$$\langle r_\pi^2\rangle|_{a\gtrsim 2} = \frac{\Gamma(1/3)}{2^{4/3}\Gamma(2/3)}\left(\frac{1}{\alpha}\right)^{2/3}\left[1+\frac{2}{3}\ln\left(\frac{a}{0.566}\right)\right]. \tag{59}$$

Using Eq. (47), we can express the coefficient in front of the square bracket in terms of f_π:

$$\langle r_\pi^2\rangle|_{a\gtrsim 2} = \frac{3}{4\pi^2 f_\pi^2} + \frac{1}{2\pi^2 f_\pi^2}\ln\left(\frac{\alpha z_0^3}{0.566}\right). \tag{60}$$

Thus, $\langle r_\pi^2\rangle$ in the $a \gtrsim 2$ region consists of two components: a fixed term $3/4\pi^2 f_\pi^2$ and a term logarithmically increasing with z_0. As $z_0 \to \infty$, the pion charge radius becomes infinite, reflecting the fact that the pion in this model is massless. A similar structure in the expression for the pion charge radius was obtained [26] in the Nambu-Jona-Lasinio (NJL) model

$$\langle r_\pi^2\rangle_{\rm NJL} = \frac{3}{2\pi^2 f_\pi^2} + \frac{1}{8\pi^2 f_\pi^2}\ln\left(\frac{m_\sigma^2}{m_\pi^2}\right). \tag{61}$$

It also has the logarithmic term $\ln m_\pi^2$ [27,28] resulting in the infinite radius for massless pion and the infrared-finite piece $3/2\pi^2 f_\pi^2$ [29,30]. The latter, however, is twice larger than that in our result (60) and contributes 0.34 fm^2 to $\langle r_\pi^2\rangle$, with the chiral logarithm term producing the extra 0.11 fm^2 required for agreement with experiment. In our case, the logarithmic term taken for $a = a_0$ is approximately equal to $3/4\pi^2 f_\pi^2$, thus almost doubling the outcome value for $\langle r_\pi^2\rangle$. More precisely, we can write

$$\langle r_\pi^2\rangle|_{a\gtrsim 2} = \frac{3}{2\pi^2 f_\pi^2}\left[1+\frac{1}{3}\ln\left(\frac{a}{2.54}\right)\right]. \tag{62}$$

For $a = 2.26$, the modified logarithmic term gives a very small contribution, and our net result is very close to the value given by the NJL fixed term. Numerically, though, this prediction of the hard-wall AdS/QCD model, as we have seen, is essentially smaller than the experimental value.

C. Form factor at large Q^2

In the large-Q^2 limit, the source $\mathcal{J}(Q, z)$ is given by its free-field version $zQK_1(Qz)$ that behaves asymptotically like e^{-Qz}. As a result, only small values $z \sim 1/Q$ are important in the form factor integral, and the large-Q^2 asymptotic behavior of the form factor is determined by the value of $\rho(z)$ at the origin [2,4,23], namely,

$$F_\pi(Q^2) \to \frac{2\rho(0)}{Q^2} = \frac{2\phi_\pi^2(0)}{Q^2} = \frac{4\pi^2 f_\pi^2}{Q^2} \equiv \frac{s_0}{Q^2}. \tag{63}$$

Note that the combination $4\pi^2 f_\pi^2 \equiv s_0 \approx 0.68$ GeV^2 frequently appears in the pion studies. In particular, it is the basic scale of the pion wave function in the local quark-hadron duality model [31,32], where it corresponds to the "pion duality interval."

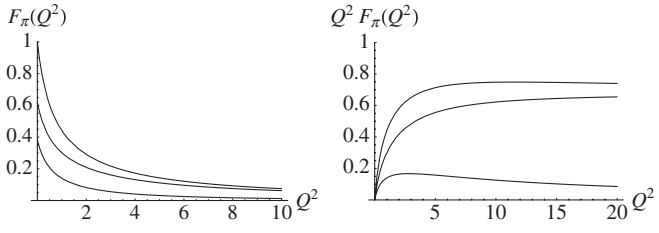

FIG. 5. Left: Contributions to pion form factor $F_\pi(Q^2)$ from Ψ^2-term (lower curve), from Φ^2-term (middle curve) and total contribution (upper curve). Right: Same for $Q^2F_\pi(Q^2)$.

The leading contribution comes entirely from the Φ^2 term of the form factor integral (41) while the Ψ^2 term contribution behaves asymptotically like $1/Q^4$ since it is accompanied by extra z^2 factor. Note, however, that it is quite visible in the experimentally interesting region $Q^2 \lesssim 10\ \mathrm{GeV}^2$ (see Fig. 5): it is responsible for more than 20% of the form factor value in this region (moreover, at $Q^2 = 0$, the Ψ^2 term contributes about 40% into the normalization of the form factor).

From a phenomenological point of view, different AdS/QCD-like models for the pion form factor differ in the shape of the density $\rho(\zeta)$ that they produce. If we require that the density $\rho(z)$ equals $2\pi^2 f_\pi^2$ at the origin, the asymptotic behavior is $F_\pi(Q^2) \to s_0/Q^2$ in any such model. For $Q^2 = 0$, the form factor is normalized to one, so basically the models would differ in how they interpolate between these two limits. In particular, the simplest interpolation is provided by the monopole formula

$$F_\pi^{\mathrm{mono}}(Q^2) = \frac{1}{1 + Q^2/s_0}, \tag{64}$$

while our hard-wall calculation gives a curve that goes above $F_\pi^{\mathrm{mono}}(Q^2)$: the ratio $F_\pi(Q^2)/F_\pi^{\mathrm{mono}}(Q^2)$ is larger than 1 for all $Q^2 > 0$, slowly approaching unity as $Q^2 \to \infty$ (see Fig. 6).

In fact, a purely monopole form factor was obtained in our paper [23], where we studied the ρ-meson form factors in the soft-wall holographic model, in which confinement is generated by $\sim z^2$ oscillator-type potential. It was shown in [23] that the form factor integral

$$\mathcal{F}(Q^2, \kappa) = \int_0^\infty dz z \mathcal{J}^{\mathrm{O}}(Q, z) |\Phi(z, \kappa)|^2, \tag{65}$$

in which $\Phi(z, \kappa) = \sqrt{2}\kappa e^{-z^2\kappa^2/2}$ is the lowest bound state wave function, and

$$\mathcal{J}^{\mathrm{O}}(Q, z) = z^2\kappa^2 \int_0^1 \frac{dx}{(1-x)^2} x^{Q^2/4\kappa^2} \exp\left[-\frac{x}{1-x} z^2\kappa^2 \right] \tag{66}$$

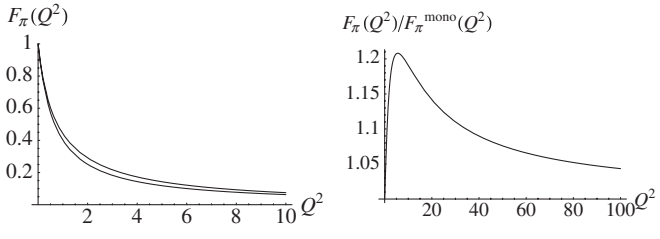

FIG. 6. Left: Pion form factor $F_\pi(Q^2)$ from the holographic model (upper curve) in comparison with the monopole interpolation $F_\pi^{\mathrm{mono}}(Q^2)$ (lower curve). Right: Ratio $F_\pi(Q^2)/F_\pi^{\mathrm{mono}}(Q^2)$.

is the bulk-to-boundary propagator of this oscillator-type model, is exactly equal to $1/(1 + Q^2/(4\kappa^2))$. The magnitude of the oscillator scale κ was fixed in our paper [23] by the value of the ρ-meson mass: $\kappa = \kappa_\rho \equiv m_\rho/2$. As a result, the form factor $\mathcal{F}(Q^2, \kappa = m_\rho/2)$ had the ρ-dominance behavior $1/(1 + Q^2/m_\rho^2)$.

If we take $\kappa = \kappa_\pi \equiv \pi f_\pi \approx 410$ MeV both for $\Phi(z, \kappa)$ and $\mathcal{J}^{\mathrm{O}}(Q, z)$, the integral (65) gives $1/(1 + Q^2/s_0)$. The relevant wave function $\Phi(z, \kappa_\pi)$ has the expected correct normalization $\Phi(0, \kappa_\pi) = \sqrt{2}\pi f_\pi$, however, the slope $1/s_0$ of $1/(1 + Q^2/s_0)$ at $Q^2 = 0$ (corresponding to $0.35\ \mathrm{fm}^2$ for the radius squared) is smaller than that of the experimental pion form factor. Furthermore, $Q^2 F_\pi^{\mathrm{mono}}(Q^2)$ tends to $s_0 \approx 0.68\ \mathrm{GeV}^2$ for large Q^2, achieving values about $0.5\ \mathrm{GeV}^2$ for $Q^2 \sim 2\ \mathrm{GeV}^2$, and thus exceeding by more than 25% the experimental JLab values [33] measured for $Q^2 = 1.6$ and $2.45\ \mathrm{GeV}^2$. The authors of Ref. [34] proposed to use Eqs. (65) and (66) as an AdS/QCD model for the pion form factor, with $\kappa = 375$ MeV chosen so as to fit these high-Q^2 data. However, such a choice underestimates the value of f_π^2 by almost 30%. Our opinion is that the AdS/QCD models should describe first the low-energy properties of hadrons, and the basic low-energy characteristics, such as m_ρ and f_π, should be used to fix the model parameters. On the other hand, if the form factor calculations based on these parameters disagree with the large-Q^2 data, it is quite possible that this is just an indication that one is using the model beyond its applicability limits. Furthermore, as we have seen in the hard-wall model, to correctly describe the pion one needs to include the chiral symmetry breaking effects absent in the vector channel. As a result, equations for pion wave functions are rather different from those in the ρ-meson case. Similarly, there are no reasons to expect that, in a soft-wall model, the pion density should have the same shape as the ρ-meson one. Unfortunately, the procedure of bringing in the chiral symmetry breaking effects that was used in the hard-wall model of Ref. [6] faces serious difficulties when applied to the AdS/QCD model [9] with the z^2 soft wall. As discussed in Ref. [9], the solution of the equation for the X field in this model requires that chiral condensate σ and the mass parameter m_q are proportional to each other, so that σ cannot be varied independently of m_q. Moreover, if one takes the chiral limit $m_q = 0$, the chiral condensate should also vanish. This difficulty may be avoided by switching to more sophisticated recent models (cf. [16–18]) in which the chiral condensate is generated dynamically. However, such a consideration goes well beyond the scope of the present paper. Thus, we just resort to an idea that whatever the mechanism is involved, the net practical outcome is a particular shape of the density $\rho(z)$ that eventually determines the pion form factor and other pion characteristics. Below, we give an example of a density $\rho^{\mathrm{mod}}(z)$ that is normalized at the origin by the experimental value of f_π,

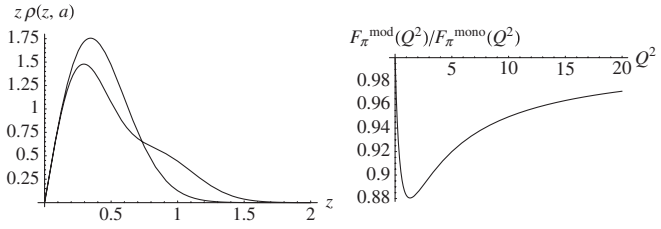

FIG. 7. Left: Model density $z\rho^{\rm mod}(z)$ (measured in fm^{-1}) is larger than the density $z|\Phi(z, \kappa_\pi)|^2$ for large z (displayed in fm). Right: Ratio $F_\pi^{\rm mod}(Q^2)/F_\pi^{\rm mono}(Q^2)$ for $B = 1/4$.

i.e., $\rho^{\rm mod}(0) = 2\kappa_\pi^2$, but which is also capable to reproduce the experimental value of the pion charge radius.

Evidently, to increase the radius, we should take a density which is larger for large z than $\Phi^2(z, \kappa = \pi f_\pi)$. Since the overall integral normalization of the density is kept fixed, this can be achieved only by decreasing the density for small z values.

Consider a simple ansatz (see Fig. 7)

$$\rho^{\rm mod}(z) = 2\kappa_\pi^2 e^{-z^2\kappa_\rho^2}[1 - Az^2\kappa_\rho^2 + Bz^4\kappa_\rho^4], \qquad (67)$$

with $A = 1 - \kappa_\rho^2/\kappa_\pi^2 + 2B$. It has both the desired value for $z = 0$ and satisfies the normalization condition

$$\int_0^\infty dz z\rho^{\rm mod}(z) = 1. \qquad (68)$$

Integrating it with $\mathcal{J}^{\rm O}(Q, z)$ taken at $\kappa = \kappa_\rho$ produces the model form factor given by the following sum of contributions of the three lowest vector states:

$$F_\pi^{\rm mod}(Q^2) = \frac{2 - (1 - 2B)s_0/m_\rho^2}{1 + Q^2/m_\rho^2} - \frac{1 - (1 - 4B)s_0/m_\rho^2}{1 + Q^2/2m_\rho^2} + \frac{2Bs_0/m_\rho^2}{1 + Q^2/3m_\rho^2}. \qquad (69)$$

The slope of $F_\pi^{\rm mod}(Q^2)$ at $Q^2 = 0$ is given by

$$\frac{dF_\pi^{\rm mod}(Q^2)}{dQ^2} = -\frac{1}{m_\rho^2}\left[\frac{3}{2} - \left(\frac{1}{2} - \frac{2}{3}B\right)\frac{s_0}{m_\rho^2}\right]. \qquad (70)$$

Taking $B = 1/4$, one obtains the experimental value 0.45 fm^2 for $\langle r_\pi^2\rangle$. It is interesting to note that the model density providing this value, has an enhancement for larger values of z (see Fig. 7), just like the pion densities in the hard-wall model (see Fig. 3). Because of a larger slope, $F_\pi^{\rm mod}(Q^2)$ decreases faster than the simple monopole interpolation $F_\pi^{\rm mono}(Q^2)$ and, as a result, is in better agreement with the data. In fact, it goes very close to $Q^2 \lesssim 1$ GeV^2 data, but exceeds the values of the JLab $Q^2 = 1.6$ and 2.45 GeV^2 points by roughly 10% and 20%, respectively.

This discrepancy has a general reason. The asymptotic AdS/QCD prediction is $Q^2F_\pi(Q^2)|_{Q^2\to\infty} \to 4\pi^2 f_\pi^2$ which is ≈ 0.68 GeV^2 for experimental value of f_π. On the other hand, JLab experimental points correspond to $Q^2F_\pi^{\rm exp}(Q^2) \approx 0.4$ GeV^2, which is much smaller than the theoretical value quoted above. The preasymptotic effects, as we have seen, reduce the discrepancy, but there still remains a sizable gap. As we already stated, such a disagreement may be just a signal that we are reaching a region where AdS/QCD models should not be expected to work. In particular, AdS/QCD models of Refs. [2,4,6,8] describe the pion in terms of an effective field or current, without specifying whether the current is built from spin-1/2 fields, or from scalar fields, etc. For Q^2 above 1 GeV^2, the quark substructure of the pion may be resolved by the electromagnetic probe (which is a widespread belief), and the description of the pion ''as a whole'' may be insufficient.

V. SUMMARY

In this paper, we studied the pion in the chiral limit of two-flavor QCD. To this end, we described a formalism that allows to extract pion form factor within the framework of the holographic dual model of QCD with hard-wall cutoff. Following Ref. [6], we identified the pion with the longitudinal component of the axial-vector gauge field. We defined two (Sturm-Liouville) conjugate wave functions $\Phi(z)$ and $\Psi(z)$ that describe the structure of the pion along the 5th dimension coordinate z. These wave functions provide a very convenient framework to study the holographic physics of the pion. We demonstrated that, just like in the ρ-meson case [22], the pion form factor is given by an integral involving the function $\rho(z)$ that has the meaning of the charge density inside the pion. However, in distinction to the ρ-case, when the density was simply given by $|\Phi(z)|^2$, the pion density has an additional term proportional to $|\Psi(z)|^2$ and entering with the z-dependent coefficient reflecting the mechanism of the spontaneous symmetry breaking. Both terms are required for normalization of the form factor at $Q^2 = 0$.

We found an analytic expression for the pion decay constant in terms of two parameters of the model: σ and z_0, similar to those used in Ref. [8]. Analyzing the results, we found it convenient to work with two combinations $\alpha = g_5\sigma/3$ and $a = \alpha z_0^3$ of the basic parameters. In particular, we found $a = a_0 = 2.26$ for the value of a corresponding to the experimental ρ-meson mass m_ρ and pion decay constant f_π. The importance of the parameter a is that its magnitude determines the regions, where the pion properties are either governed by the confinement effects or by the effects from the spontaneous chiral symmetry breaking. For example, in the practically important domain $a > 2$, the pion decay constant is determined primarily by σ, with negligibly tiny corrections due to z_0 value. However, when $a < 1$ the pion decay constant is proportional to the ratio a/z_0. Besides, for small $a \ll 1$, the radius of the pion is given by $\langle r_\pi^2\rangle = \frac{4}{3}z_0^2$, i.e., as one may expect, the pion size is completely determined by

the confinement radius. On the other hand, for $a > 2$ the radius is basically determined by $1/\sigma^{1/3}$, slowly increasing with z_0 due to the $\ln a/a_0$ correction.

We also found that the pion rms charge radius $\langle r_\pi^2 \rangle^{1/2} \approx 0.58$ fm in the hard-wall model is smaller than that measured experimentally. In a sense, the hard wall at the distance $z_0 \approx 0.62$ fm (fixed from the ρ-meson mass), "does not allow" the pion to get larger. So, we argued that if the IR wall is "softened," the size of the pion may be increased by an amount sufficient to accommodate the data. A straightforward idea is to use the soft-wall model of Ref. [9] and treat the pion in a way similar to what was done in [23] for the ρ-meson case. Unfortunately, there are prohibiting complications with directly introducing the chiral symmetry effects within the AdS/QCD model with the z^2 soft wall. As explained in Ref. [9], the chiral condensate σ in such a model is proportional to the mass parameter m_q, so that in the chiral limit the condensate vanishes together with the quark mass.

To illustrate a possible change in the form factor predictions due to the softening of the IR wall, we proposed an ansatz for the pion density function and used the vector current source from the soft-wall model considered in Ref. [23]. We demonstrated that this ansatz is capable to fit the experimental value of the pion charge radius. It also closely follows the data in the $Q^2 < 1$ GeV^2 region, while still overshoots available data in the $Q^2 \sim 2$ GeV^2 region. The basic source of this discrepancy is very general: the asymptotic AdS/QCD prediction for the pion form factor is $Q^2 F_\pi(Q^2) \to 4\pi^2 f_\pi^2$, and if one takes the experimental value for f_π, one obtains $Q^2 F_\pi(Q^2) \to 0.68$ GeV^2, which is much larger than the 0.4 GeV^2 value given by $Q^2 \sim 2$ GeV^2 JLab data. For this reason, we argued that the disagreement mentioned above may be a signal that the region $Q^2 \gtrsim 2$ GeV^2 is beyond the applicability region of AdS/QCD models.

Finishing the write-up of this paper, we have learned that the paper [35] addressing the same problem was posted into the arxive. We did not observe, however, essential overlaps with our ideas and results.

ACKNOWLEDGMENTS

H. G. would like to thank A. W. Thomas for valuable comments and support at Jefferson Laboratory, J. P. Draayer for support at Louisiana State University.

Notice: Authored by Jefferson Science Associates, LLC under U.S. DOE Contract No. DE-AC05-06OR23177. The U.S. Government retains a nonexclusive, paid-up, irrevocable, worldwide license to publish or reproduce this manuscript for U.S. Government purposes.

[1] J. M. Maldacena, Adv. Theor. Math. Phys. **2**, 231 (1998); Int. J. Theor. Phys. **38**, 1113 (1999); S. S. Gubser, I. R. Klebanov, and A. M. Polyakov, Phys. Lett. B **428**, 105 (1998); E. Witten, Adv. Theor. Math. Phys. **2**, 253 (1998).
[2] J. Polchinski and M. J. Strassler, Phys. Rev. Lett. **88**, 031601 (2002); J. High Energy Phys. 05 (2003) 012.
[3] H. Boschi-Filho and N. R. F. Braga, J. High Energy Phys. 05 (2003) 009; Eur. Phys. J. C **32**, 529 (2004).
[4] S. J. Brodsky and G. F. de Téramond, Phys. Lett. B **582**, 211 (2004); G. F. de Teramond and S. J. Brodsky, Phys. Rev. Lett. **94**, 201601 (2005).
[5] T. Sakai and S. Sugimoto, Prog. Theor. Phys. **113**, 843 (2005); **114**, 1083 (2005).
[6] J. Erlich, E. Katz, D. T. Son, and M. A. Stephanov, Phys. Rev. Lett. **95**, 261602 (2005).
[7] J. Erlich, G. D. Kribs, and I. Low, Phys. Rev. D **73**, 096001 (2006).
[8] L. Da Rold and A. Pomarol, Nucl. Phys. **B721**, 79 (2005); J. High Energy Phys. 01 (2006) 157.
[9] A. Karch, E. Katz, D. T. Son, and M. A. Stephanov, Phys. Rev. D **74**, 015005 (2006).
[10] C. Csaki and M. Reece, J. High Energy Phys. 05 (2007) 062.
[11] T. Hambye, B. Hassanain, J. March-Russell, and M. Schvellinger, Phys. Rev. D **74**, 026003 (2006); arXiv:hep-ph/0612010.
[12] J. Hirn and V. Sanz, J. High Energy Phys. 12 (2005) 030; J. Hirn, N. Rius, and V. Sanz, Phys. Rev. D **73**, 085005 (2006).
[13] K. Ghoroku, N. Maru, M. Tachibana, and M. Yahiro, Phys. Lett. B **633**, 602 (2006).
[14] S. J. Brodsky and G. F. de Teramond, Phys. Rev. Lett. **96**, 201601 (2006).
[15] N. Evans, A. Tedder, and T. Waterson, J. High Energy Phys. 01 (2007) 058.
[16] R. Casero, E. Kiritsis, and A. Paredes, arXiv:hep-th/0702155.
[17] U. Gursoy and E. Kiritsis, arXiv:0707.1324.
[18] U. Gursoy, E. Kiritsis, and F. Nitti, arXiv:0707.1349.
[19] O. Bergman, S. Seki, and J. Sonnenschein, arXiv:0708.2839.
[20] J. Erdmenger, K. Ghoroku, and I. Kirsch, J. High Energy Phys. 09 (2007) 111.
[21] A. Dhar and P. Nag, arXiv:0708.3233.
[22] H. R. Grigoryan and A. V. Radyushkin, Phys. Lett. B **650**, 421 (2007).
[23] H. R. Grigoryan and A. V. Radyushkin, Phys. Rev. D **76**, 095007 (2007).
[24] A. V. Radyushkin, Phys. Lett. B **642**, 459 (2006).
[25] S. Eidelman *et al.* (Particle Data Group), Phys. Lett. B **592**, 1 (2004).
[26] H. J. Hippe, Phys. Rev. C **52**, 2172 (1995).

[27] M. A. B. Beg and A. Zepeda, Phys. Rev. D **6**, 2912 (1972).
[28] M. K. Volkov and V. N. Pervushin, Phys. Lett. **51B**, 356 (1974).
[29] S. B. Gerasimov, Yad. Fiz. **29**, 513 (1979) [Sov. J. Nucl. Phys. **29**, 259 (1979)].
[30] V. Bernard and D. Vautherin, Phys. Rev. D **40**, 1615 (1989).
[31] A. V. Radyushkin, Acta Phys. Pol. B **26**, 2067 (1995).
[32] V. A. Nesterenko and A. V. Radyushkin, Phys. Lett. **115B**, 410 (1982).
[33] T. Horn *et al.* (Fpi2 Collaboration), Phys. Rev. Lett. **97**, 192001 (2006).
[34] S. J. Brodsky and G. F. de Teramond, arXiv:0707.3859.
[35] H. J. Kwee and R. F. Lebed, arXiv:0708.4054.